

Supporting Information

Oxidation of 8-oxo-7,8-dihydro-2'-deoxyguanosine leads to substantial DNA-histone cross-links within nucleosome core particles

Jing Bai,¹ Yingqian Zhang,¹ Zhen Xi,¹ Marc M. Greenberg³ and Chuanzheng Zhou^{1,2,*}

¹ State Key Laboratory of Elemento-Organic Chemistry and Department of Chemical Biology, College of Chemistry, Nankai University, Tianjin 300071, China

² Collaborative Innovation Center of Chemical Science and Engineering (Tianjin), Tianjin 300071, China

³ Department of Chemistry, Johns Hopkins University, 3400 N. Charles St., Baltimore, MD 21218, USA

* Corresponding author: Chuanzheng Zhou. Email: chuanzheng.zhou@nankai.edu.cn

Contents:

Figure S1. Preparation of 145 nt singl-stranded 601 DNA by ligation. (S3)

Figure S2. 5% nondenaturing PAGE analysis of the formation and stability of NCPs. (S4)

Figure S3. 10% SDS PAGE analysis of histone octamers treated with different concentrations of Na_2IrCl_6 , Na_2IrBr_6 and $\text{K}_3\text{Fe}(\text{CN})_6$. (S5)

Figure S4. Representative gels of DPC formation and DNA scission in NCPs containing wide type histones. (S8)

Figure S5. Kinetics of 8-oxodGuo oxidation and DPC formation in NCPs containing wide type histones. (S9)

Figure S6. Protein identification though MS/MS analysis of tryptic peptide fragments of DPC generated from NCP-8-oxodGuo⁸⁹/C. (S11)

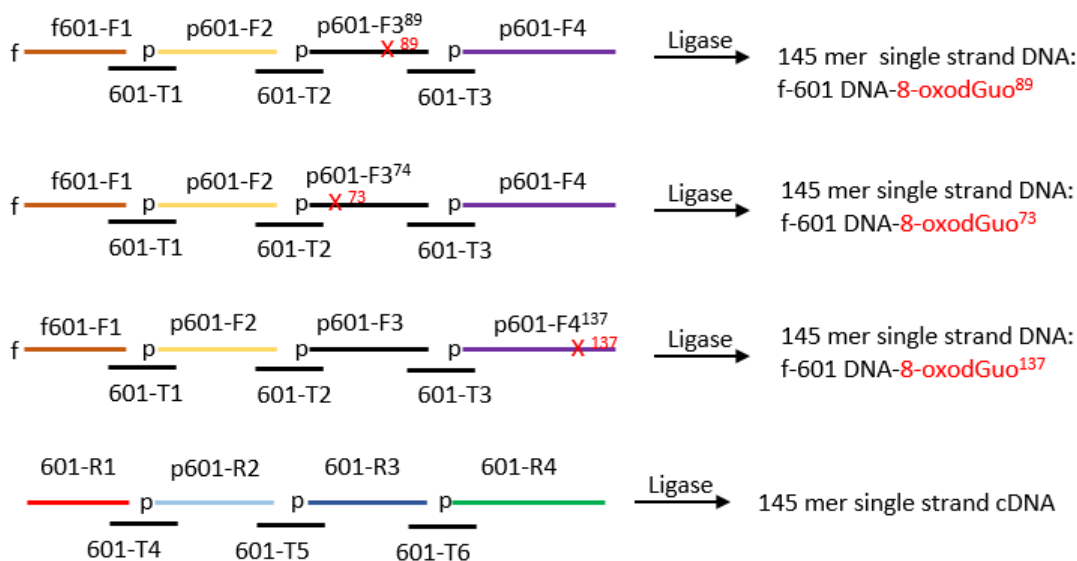
Figure S7. Kinetics of 8-oxodGuo oxidation and DPC formation in NCP-8-oxodGuo⁸⁹/C containing mutated histone H4. (S12)

Figure S8. Representative gels of DPC formation and DNA scission in NCP-8-oxodGuo⁸⁹/C containing mutated histone H4. (S15)

Figure S9. Representative gels of DPC formation in NCP-8-oxodGuo⁸⁹/T in the presence of 1 mM spermine. (S16)

(f601-F1) (FAM)-ATCGATGTATATATCTGACACGTGCCTGGA (30 nt)
 (p601-F2) pGACTAGGGAGTAATCCCCCTTGGCGGTTAAAACGCG (35 nt)
 (p601-F3) pGGGGACAGCGCGTACGTGCGTTTGAGCGGTGCTAG (35 nt)
 (p601-F3⁸⁹) pGGGGACAGCGCGTACGTGCGTTT X⁸⁹AGCGGTGCTAG (35 nt)
 (p601-F3⁷³) pGGGGACAX⁷³CGCGTACGTGCGTTTGAGCGGTGCTAG (35 nt)
 (p601-F4) pAGCTGTCTACGACCAATTGAGCGGCCTCGGCACCGGGATTCTGAT (45 nt)
 (p601-F4¹³⁷) pAGCTGTCTACGACCAATTGAGCGGCCTCGGCACCGGX¹³⁷ATTCTGAT (45 nt)
 (601-T1) CTCCCTAGTCTCCAGGCACG (20 nt)
 (601-T2) CGCTGTCCCCCGCGTTTTAA (20 nt)
 (601-T3) GTAGACAGCTCTAGCACCGC (20 nt)

(Zhou-R1) ATCAGAATCCCGGTGCCGAGGCCGCTCAATTGGTC (35 nt)
 (pZhou-R2) pGTAGACAGCTCTAGCACCGCTCAAACGCAC (30 nt)
 (pZhou-R3) pGTACGCGCTGTCCCCCGCGTTTTAACCGCCAAGGG (35 nt)
 (pZhou-R4) pGATTACTCCCTAGTCTCCAGGCACGTGTCAGATATATACATCGAT (45 nt)
 (601-T4) AGCTGTCTACGACCAATTGA (20 nt)
 (601-T5) CAGCGGTACGTGCGTTTGA (20 nt)
 (601-T6) GGGAGTAATCCCCCTTGGCGG (20 nt)
 (601-T7) CGCTGAAACGCACGTACG CG (20 nt)



Sequence of 145 nt single-stranded 601 DNA:

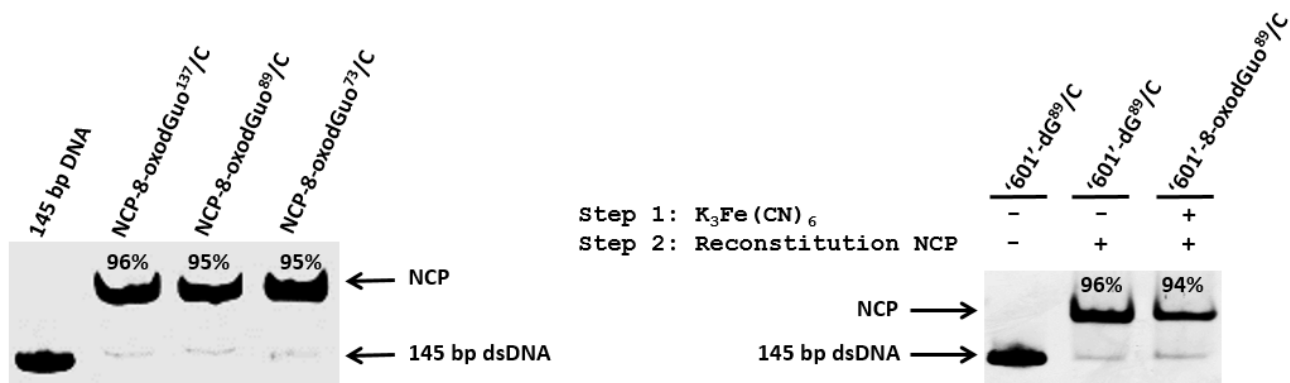
5' (FAM) ATCGATGTATATATCTGACACGTGCCTGGAGACTAGGGAGTAATCCCCCTTGGCGGTTAAAACGCGGGGGACAG⁷³GGCGTACG
 TGCGTTTG⁸⁹AGCGGTGCTAGAGCTGTCTACGACCAATTGAGCGGCCTCGGCACCGGG¹³⁷ATTCTGAT 3'

Sequence of 145 nt single-stranded 601 cDNA:

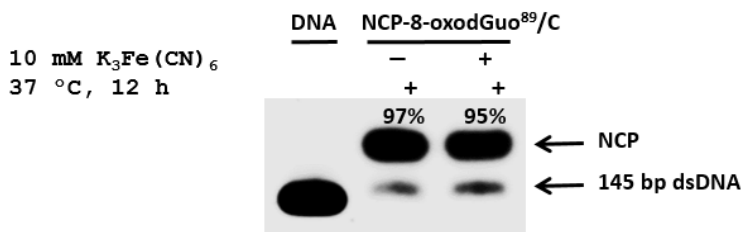
3' AGCTACATATATAGACTGTGCACGGACCTCTGATCCCTCATTAGGGGAACCGCCAATTTGCGCCCCCTGTGCGCATGCACGCAAAC
 TCGCCACGATCTCGACAGATGCTGGTTAACTCGCCGGAGCCGTGGCCCTAAGACTA 5' (cDNA)

Figure S1. Preparation of 145 nt single-stranded 601 DNA by ligation. “X” denotes 8-oxodGuo. “f” denote 5’-FAM labeling. “p” denotes 5’-phosphate group.

(S2A) Electrophoretic mobility shift assay showing the efficiency of NCP reconstitutions



(S2B) Electrophoretic mobility shift assay showing the stability of NCP upon 10 mM $K_3Fe(CN)_6$ treatment



(S2C) Electrophoretic mobility shift assay showing the stability of NCP upon heat treatment

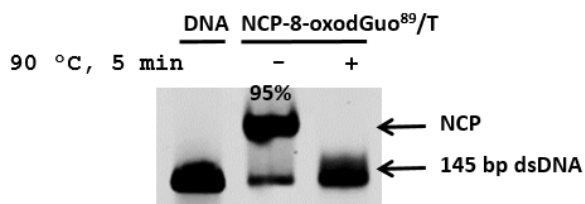


Figure S2. 5% (w/v) nondenaturing PAGE analysis of the formation and stability of NCPs.

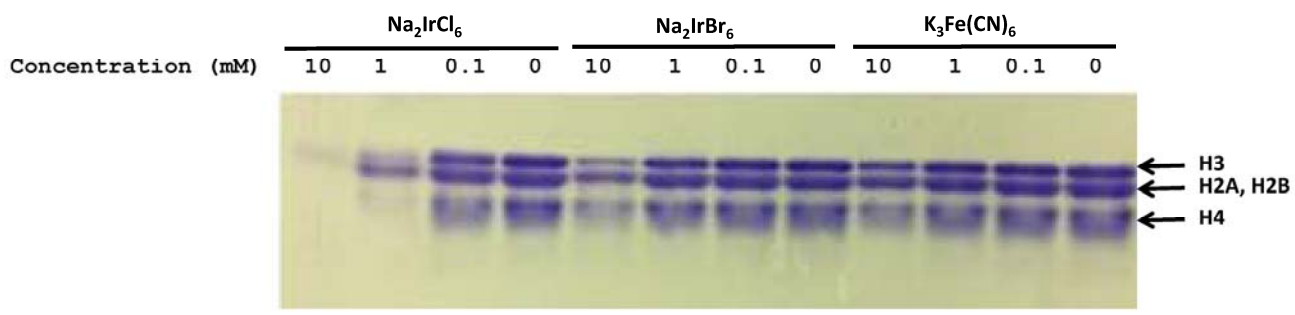
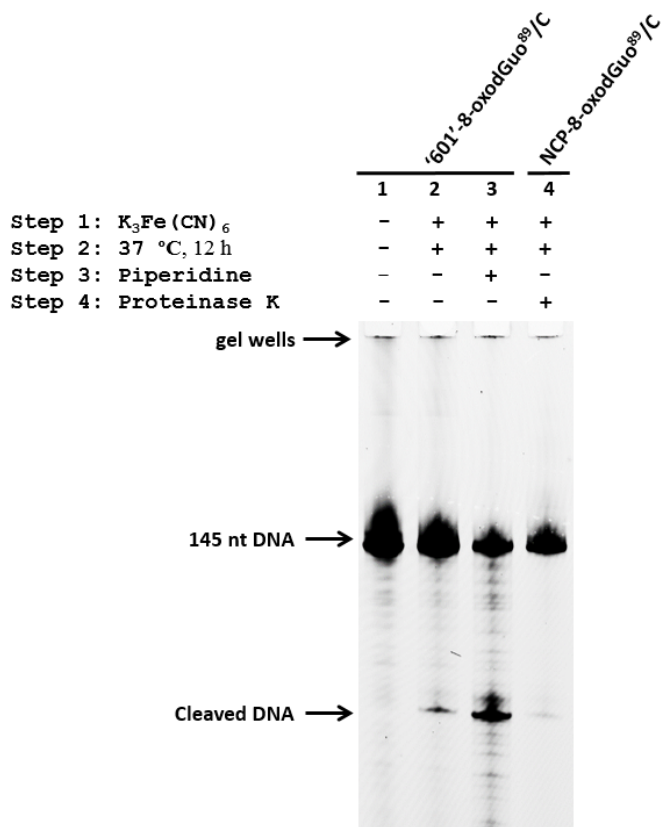
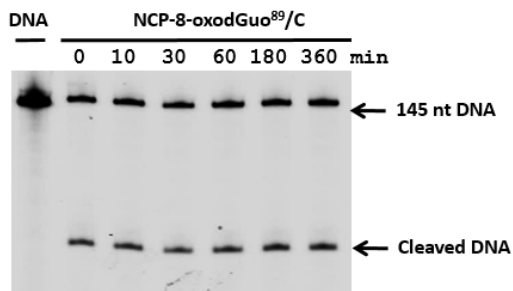


Figure S3. 10% (w/v) SDS PAGE analysis of histone octamers treated with different concentrations of Na_2IrCl_6 , Na_2IrBr_6 and $\text{K}_3\text{Fe}(\text{CN})_6$.

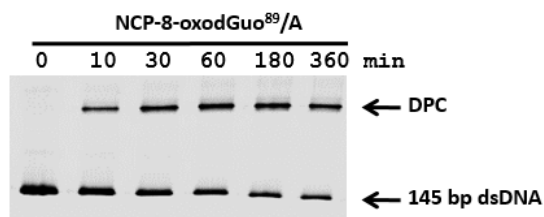
(S4A) 8% (w/v) denaturing PAGE analysis of reactions of NCP-8-oxodGuo⁸⁹/C and free DNA '601'-8-oxodGuo⁸⁹/C upon K₃Fe(CN)₆ oxidation



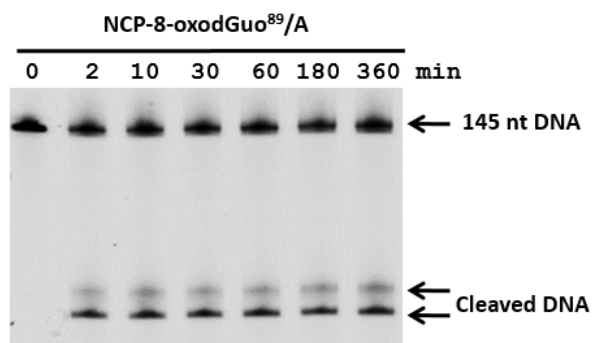
(S4B) 8% (w/v) denaturing PAGE analysis of DNA scission in NCP-8-oxodGuo⁸⁹/C upon K₃Fe(CN)₆ oxidation



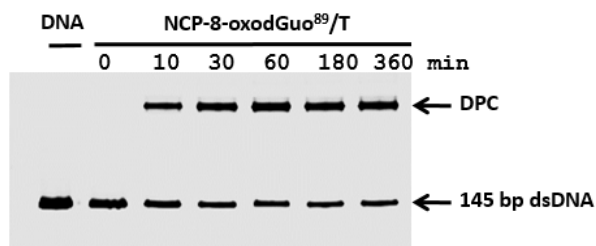
(S4C) 10% (w/v) SDS PAGE analysis of DPC formation in NCP-8-oxodGuo⁸⁹/A upon K₃Fe(CN)₆ oxidation



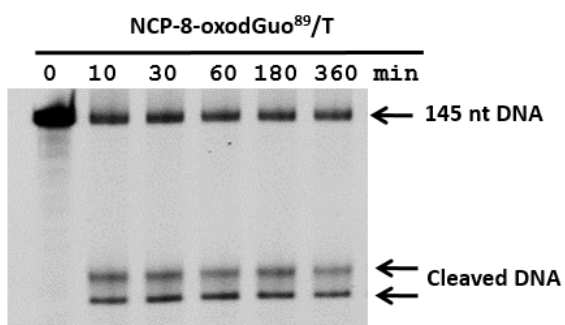
(S4D) 8% (w/v) denaturing PAGE analysis of DNA scission in NCP-8-oxodGuo⁸⁹/A upon K₃Fe(CN)₆ oxidation



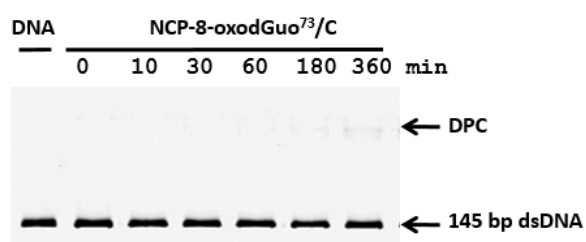
(S4E) 10% (w/v) SDS PAGE analysis of DPC formation in NCP-8-oxodGuo⁸⁹/T upon K₃Fe(CN)₆ oxidation



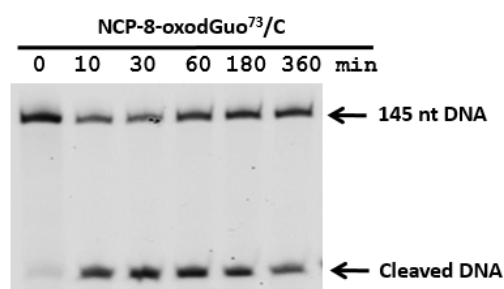
(S4F) 8% (w/v) denaturing PAGE analysis of DNA scission in NCP-8-oxodGuo⁸⁹/T upon K₃Fe(CN)₆ oxidation



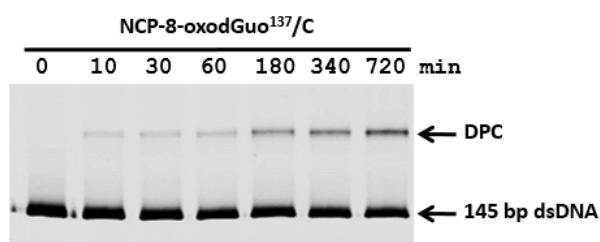
(S4G) 10% (w/v) SDS PAGE analysis of DPC formation in NCP-8-oxodGuo⁷³/C upon K₃Fe(CN)₆ oxidation



(S4H) 8% (w/v) denaturing PAGE analysis of DNA scission in NCP-8-oxodGuo⁷³/C upon K₃Fe(CN)₆ oxidation



(S4I) 10% (w/v) SDS PAGE analysis of DPC formation in NCP-8-oxodGuo¹³⁷/C upon K₃Fe(CN)₆ oxidation



(S4J) 8% (w/v) denaturing PAGE analysis of DNA scission in NCP-8-oxodGuo¹³⁷/C upon K₃Fe(CN)₆ oxidation

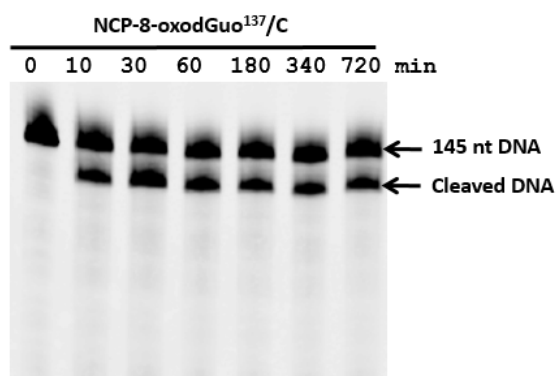


Figure S4. Representative gels of DPC formation and DNA scission in NCPs containing wide type histones.

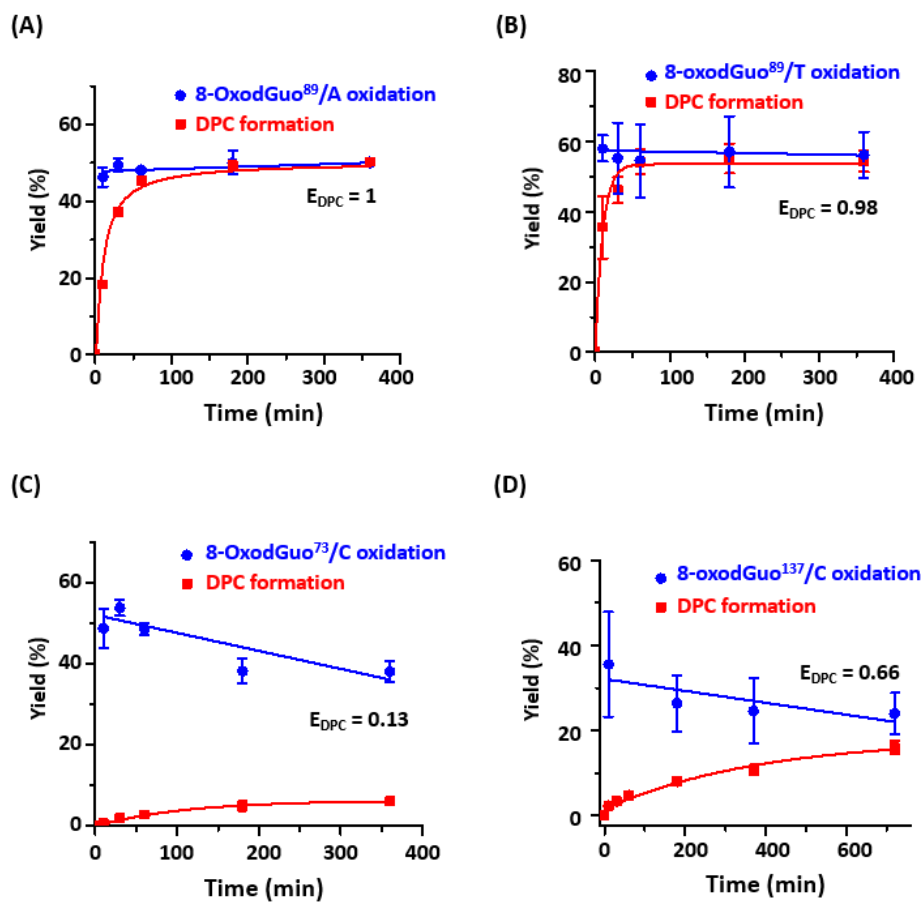
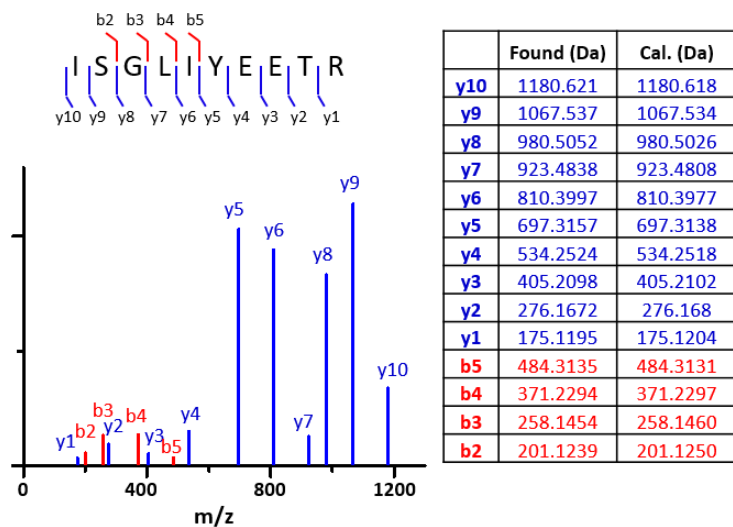
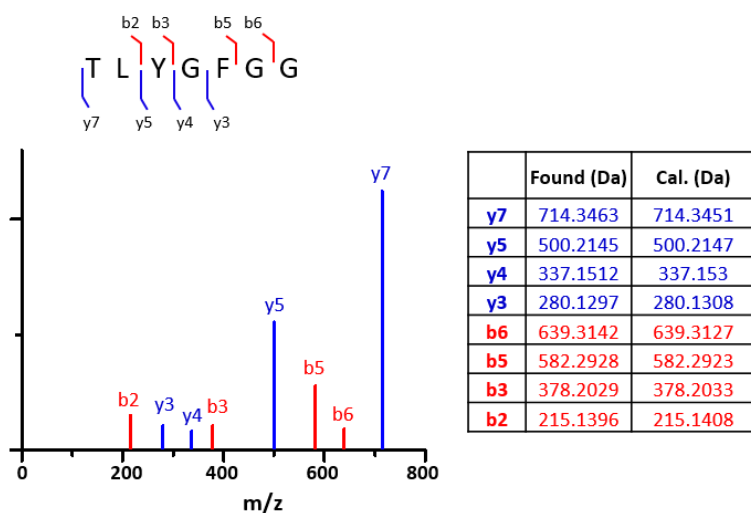


Figure S5. Kinetics of 8-oxodGuo oxidation and DPC formation in NCPs containing wide type histones. (A) NCP-8-oxodGuo⁸⁹/A; (B) NCP-8-oxodGuo⁸⁹/T; (C) NCP-8-oxodGuo⁷³/C; (D) NCP-8-oxodGuo¹³⁷/C.

(S6A) Identified fragment ISGLIYEETR of H4



(S6B) Identified fragment TLYGFGG of H4



(S6C) Identified fragment VFLENVIR of H4

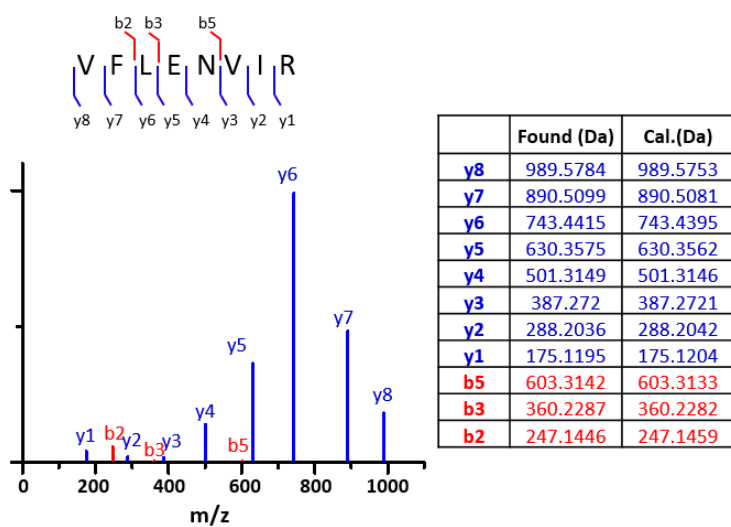


Figure S6 Protein identification through MS/MS analysis of tryptic peptide fragments of DPC generated from NCP-8-oxodGuo⁸⁹/C.

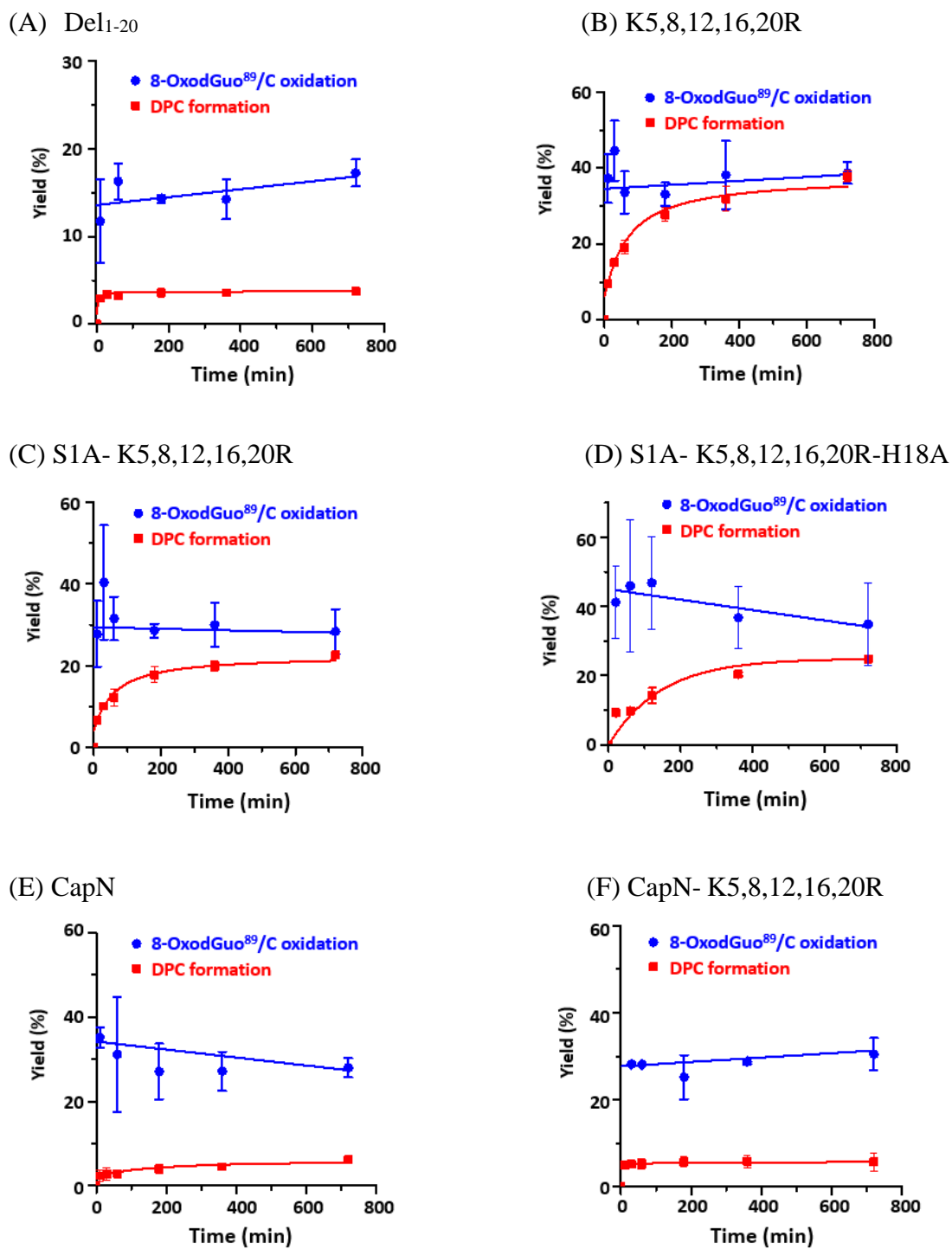
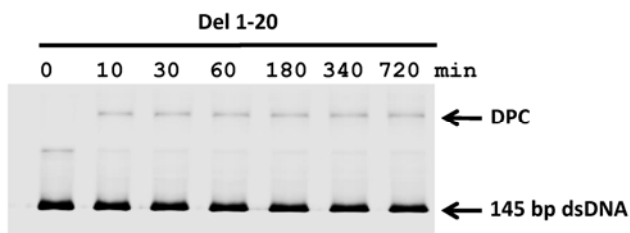
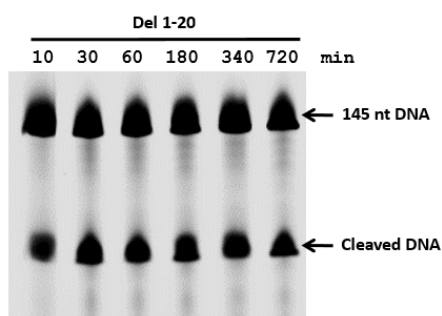


Figure S7. Kinetics of 8-oxodGuo oxidation and DPC formation in NCP-8-oxodGuo⁸⁹/C containing mutated histone H4.

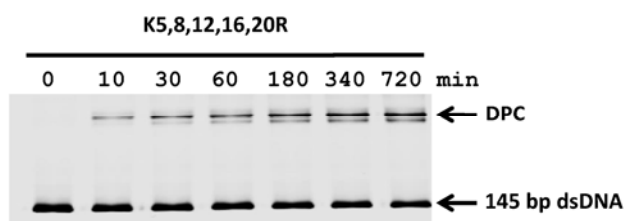
(S8A) 10% (w/v) SDS PAGE analysis of DPC formation in NCP-8-oxodGuo⁸⁹/C containing H4-Del₁₋₂₀ mutant



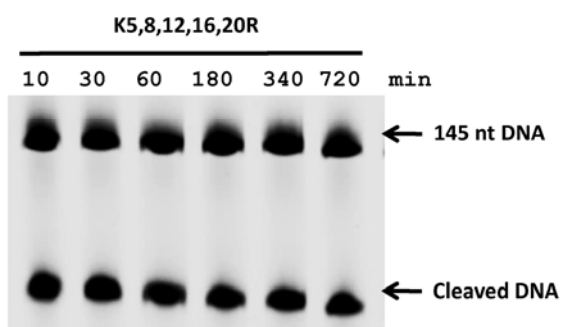
(S8B) 8% (w/v) denaturing PAGE analysis of DNA scission in NCP-8-oxodGuo⁸⁹/C containing H4-Del₁₋₂₀ mutant



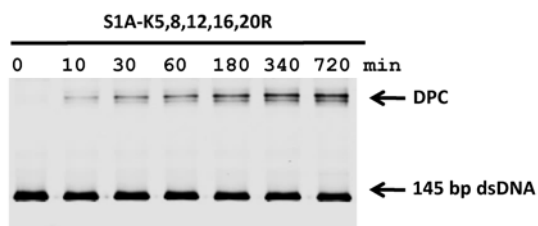
(S8C) 10% (w/v) SDS PAGE analysis of DPC formation in NCP-8-oxodGuo⁸⁹/C containing H4-K5,8,12,16,20R mutant



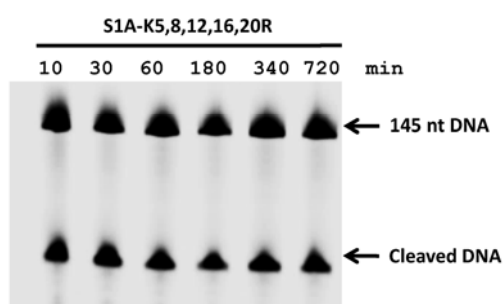
(S8D) 8% (w/v) denaturing PAGE analysis of DNA scission in NCP-8-oxodGuo⁸⁹/C containing H4-K5,8,12,16,20R mutant



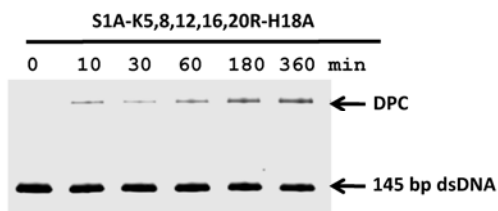
(S8E) 10% (w/v) SDS PAGE analysis of DPC formation in NCP-8-oxodGuo⁸⁹/C containing H4-S1A-K5,8,12,16,20R mutant



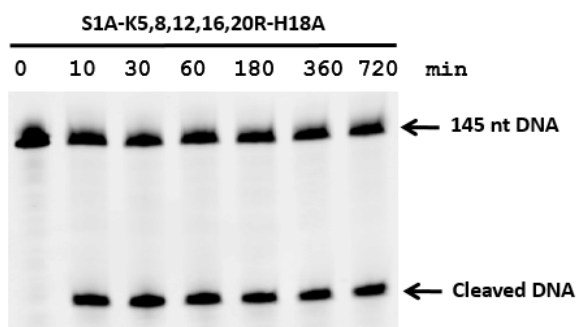
(S8F) 8% (w/v) denaturing PAGE analysis of DNA scission in NCP-8-oxodGuo⁸⁹/C containing H4-S1A-K5,8,12,16,20R mutant



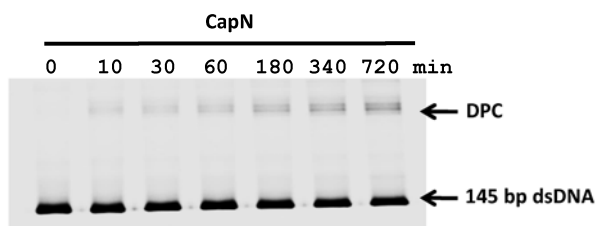
(S8G) 10% (w/v) SDS PAGE analysis of DPC formation in NCP-8-oxodGuo⁸⁹/C containing H4-S1A-K5,8,12,16,20R-H18A mutant



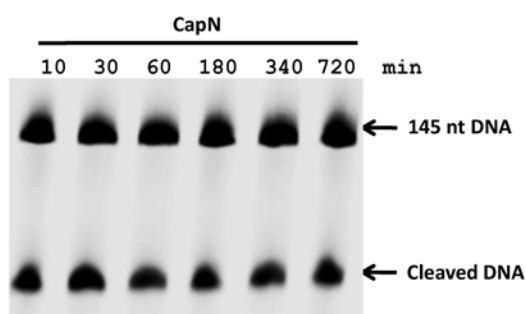
(S8H) 8% (w/v) denaturing PAGE analysis of DNA scission in NCP-8-oxodGuo⁸⁹/C containing H4-S1A-K5,8,12,16,20R-H18A mutant



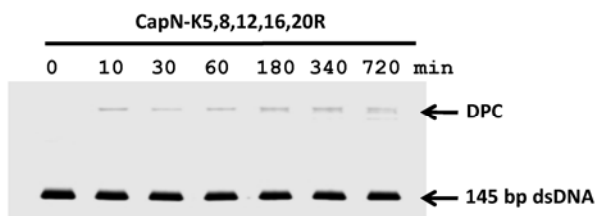
(S8I) 10% (w/v) SDS PAGE analysis of DPC formation in NCP-8-oxodGuo⁸⁹/C containing H4-CapN mutant



(S8J) 8% (w/v) denaturing PAGE analysis of DNA scission in NCP-8-oxodGuo⁸⁹/C containing H4-CapN mutant



(S8K) 10% (w/v) SDS PAGE analysis of DPC formation in NCP-8-oxodGuo⁸⁹/C containing H4-CapN- K5,8,12,16,20R mutant



(S8L) 8% (w/v) denaturing PAGE analysis of DNA scission in NCP-8-oxodGuo⁸⁹/C containing H4-CapN- K5,8,12,16,20R mutant

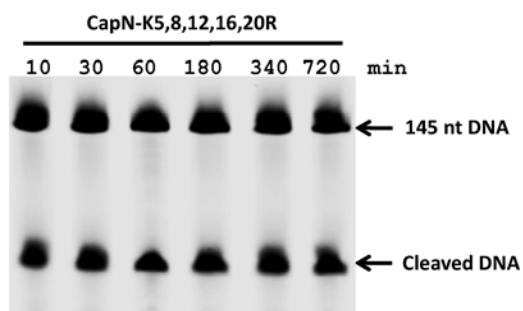
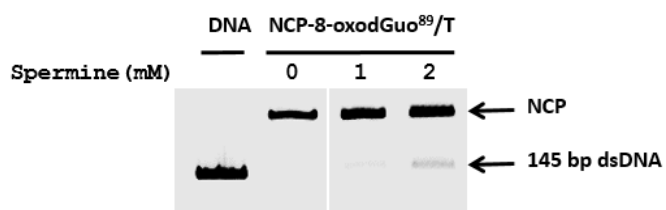


Figure S8. Representative gels of DPC formation and DNA scission in NCP-8-oxodGuo⁸⁹/C containing mutated histone H4.

(A) 5% (w/v) nondenaturing PAGE analysis of the stability of NCP upon spermine treatment



(B) 10% (w/v) SDS PAGE analysis of DPC formation in the presence of spermine

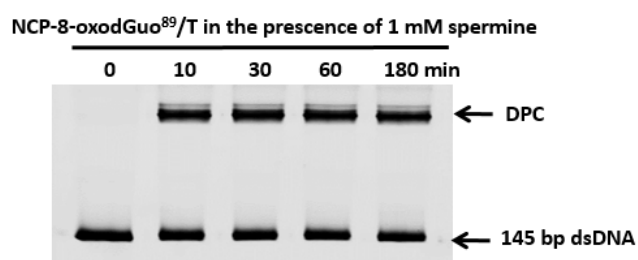


Figure S9. Representative gels of DPC formation in NCP-8-oxodGuo⁸⁹/T in the presence of 1 mM spermine.